Spray Combustion Simulation in Transverse Injecting Configurations

Yoon-Yong Yi and Tae-Seong Roh
Inha University
YongHyun-Dong 253, Nam-Gu, Incheon, Korea
navi1994@lycos.co.kr

Abstract

The reactive flowfield of the transverse injecting combustor has been studied using Euler-Lagrange method in order to develop an efficient solution procedure for the understanding of liquid spray combustion in the transverse injecting combustor which has been widely used in ramjets and turbojet afterburners. The unsteady two-dimensional gas-phase equations have been represented in Eulerian coordinates and the liquid-phase equations have been formulated in Lagrangian coordinates. The gas-phase equations based on the conservation of mass, momentum, and energy have been supplemented by combustion. The vaporization model takes into account the transient effects associated with the droplet heating and the liquid-phase internal circulation. The droplet trajectories have been determined by the integration of the Lagrangian equation in the flowfield obtained from the separate calculation without considering the iterative effect between liquid and gas phases. The reported droplet trajectories had been found to deviate from the initial conical path toward the flow direction in the very end of its lifetime when the droplet size had become small due to evaporation. The integration scheme has been based on the TEACH algorithm for gas-phase equation, the second order Runge-Kutta method for liquid-phase equations and the linear interpolation between the two coordinate systems. The calculation results has shown that the characteristics of the droplet penetration and recirculation have been strongly influenced by the interaction between gas and liquid phases in such a way that most of the vaporization process has been confined to the wake region of the injector, thereby improving the flame stabilization properties of the flowfield.

1. Introduction

The spray combustion has been used extensively in engineering application, including industrial boilers, ramjet combustors, liquid propellant rocket engines and aircraft propulsion systems. The aerodynamic flow pattern, the flame properties and heat transfer have been the important characteristics in such application. A computational method has been one of the useful techniques for designing or optimizing the more efficient combustion device. Extensive reviews of spray combustion can be found in Refs.[1-5]. In treating the droplet-phase for modeling dilute spray

combustion, the numerical models can be classified into three kinds according to the treatment of inter-phase transport rates. The first is the locally homogeneous flow model (LHF), in which the inter-phase transport rates are assumed to be infinitely fast. The droplet and gas-phase are assumed to be in kinetic and thermodynamic equilibrium at each point in the flow. Hence, there is no velocity slip or temperature difference between the droplet and gas-phase. This can be identified as a single fluid model and can only be used to simulate the small droplet spray combustion. The second model is known as the deterministic separated flow model (DSF), in which the droplet temperature and velocity are solved along the droplet trajectory, independent of the gas-phase turbulence. The droplet trajectory is a time-averaged trajectory and the effect of spray droplet on gas-phase turbulence is also ignored in this model. The third model is the stochastic separated flow model (SSF), in which both finite inter-phase transport rates and effect of turbulence interactions between droplet and gas-phase are considered. This model has been commonly used in various spray combustion modeling by many researchers such as Crowe et al. [6] and Shuen [7]. Both the DSF model and the SSF model adopt Eulerian gas and Lagrangian droplet formulation. By using the Lagrangian treatment of droplets, it is easy to calculate the evaporation history and temperature change of a single droplet. However, in order to obtain a detailed distribution of the droplet velocity and concentration for comparison with experimental data, a large amount of droplet trajectories are required.

In this paper, the DSF model for the simulation of the dilute spray combustion has been developed, using the Eulerian treatment for the gas-phase and the Lagrangian treatment for the droplet liquid phase. The changes of the droplet mass and diameter due to evaporation, the temperature due to heat exchange, and the velocity due to gas-phase flow have been described by ordinary differential equations. Other gas-phase equations have been described by partial in Eulerian coordinates.

2. Gas-Phase Equations

The governing equations based on the conservation of the gas phase flow properties are generally in elliptic in space and parabolic in time. The gas phase equations in Eulerian coordinate can be expressed in the following.

Table 1 Source terms appearing equation (1)

Equation	ϕ	Γ_ϕ	$S_{\phi,g}$	$S_{\phi,l}$
Continuity	1	0	0	$-\sum n_k \dot{m}_k$
Momentum	v_i	μ_e	$-\frac{\partial P}{\partial x_i} + \frac{\partial}{\partial x_j}\left(\Gamma_\phi \frac{\partial v_j}{\partial x_i}\right) + \frac{\partial}{\partial x_j}\left(\Gamma_\phi \frac{\partial v_i}{\partial x_j}\right) + \rho g_i$	$\sum\{n_k \dot{m}_k u_i - \beta_k(u_i - v_k)\}$
Species mass fraction	Y_s		$-W_s$	$-\alpha_s \sum n_k \dot{m}_k$
Energy	h	$\frac{\mu_e}{\sigma_h}$	$W_s Q_s + n_k \dot{m}_k L$	$-\sum n_k L - \sum n_k \dot{m}_k C_{p,k} T_k$
Turbulent kinetic energy	k	$\frac{\mu_e}{\sigma_\varepsilon}$	$G_k - \rho\varepsilon$	0
Dissipation rate	ε	$\frac{\mu_e}{\sigma_\varepsilon}$	$\frac{\varepsilon}{k}(C_1 G_k - C_2 \rho\varepsilon)$	0

$$\frac{\partial}{\partial x_j}(\rho u_j \phi) = \frac{\partial}{\partial x_j}\left(\Gamma_\phi \frac{\partial \phi}{\partial x_j}\right) + S_{\phi,g} + S_{\phi,l} \qquad (1)$$

where ϕ is the independent variable, Γ_ϕ is the effective transport coefficient, $S_{\phi,g}$ is the gas-phase source term per unit volume and $S_{\phi,l}$ is the liquid droplet phase source term. Table 1 contains all the relevant information pertaining to each of the dependent variables. The gas phase equations are nondimensionalized using the inflow conditions of the combustor held fixed in time for the calculations presented. The length scales are converted to be dimensionless with respect to the combustor diameter. The turbulent shear stresses are evaluated using the $k-\varepsilon$ model of Launder and Spalding.[9] The combustion model is based on the analogy that no envelope flame is present and the individual droplet acts as a source of fuel vapor for the gas phase. The reaction rate is determined by taking into account the minimum of either reaction rate obtained from the eddy breakup model of Spalding[10] or the Arrhenius reaction rate based on a single-step reaction mechanism given by Westbrook and Dryer.[11]

$$W_s = w_f \min\left\{\begin{array}{l} A\left(\dfrac{\rho Y_f}{W_f}\right)^a \left(\dfrac{\rho Y_o}{W_o}\right)^b \exp\left(\dfrac{-E}{RT}\right), \\[2mm] \dfrac{C_R}{W_f} g^{1/2}\left(\dfrac{\rho\varepsilon}{k}\right) \end{array}\right\} \qquad (2)$$

In the present calculations, a special form of the conservation equation based on energy involving $C_p(T)$ and T is employed. The specific heat of the mixture is given by

$$C_p(T) = \sum_i y_i C_{p,i}(T) \qquad (3)$$

with summation over all species. The chemical kinetics are modeled by single step kinetic mechanisms, where each component of the fuel reacts separately with oxidizer to form products.

By assuming equal binary diffusion coefficients for all the species and by knowing the mass fractions of fuel and oxidizer and the stoichiometric relationship of the given hydrocarbon-air mixture, the mass fractions of the remaining species N_2, CO_2 and H_2O can be easily determined in terms of simple algebraic expressions. The variation of the specific heats with temperature is considered by using polynomials of the form

$$C_{p,i} = \frac{R}{W_i}(C_{1i} + C_{2i}T + C_{3i}T^2 + C_{4i}T^3 + C_{5i}T^4) \qquad (4)$$

The constants in the polynomials are complied from CRC[12]. The system of equations for the gas phase is completed with the following equation of state:

$$\rho = (v_c - 1)M_c^2 \frac{p}{RT\sum_i \frac{y_i}{W_i}} \qquad (5)$$

For the equations involving mass fraction of fuel, oxidizer, and concentration fluctuation, the flux normal to the wall is set to zero. Inflow boundary conditions for all dependent variables are prescribed. The radial velocity is set to zero at the axis of symmetry. All other boundary conditions are based on normal gradients, which are set to be zero at the axis of symmetry and the outflow.

3. Liquid-Phase Equations

Among the various advantages of using the Lagrange formulation for the liquid-phase equations are its ability to handle multi-valuedness of solutions in a natural way, elimination of numerical diffusion, and restriction of the Lagrangian calculations to the region where droplets are existing so that the Eulerian-Lagrangian approach can be used for the very fine resolution required.[4,5] The main assumptions of the liquid-phase equations are followed,

1. The evaluation process is quasi-steady.

2. Fuel and oxidizer react in stoichiometric proportion at the flame.
3. Effect of turbulent fluctuation of gas velocity and mass fractions on droplet is negligible.
4. Radiation heat transfer is negligible.
5. The Lewis number is unity.

The liquid-phase and gas-phase equations are nondimensionalized with respect to the same scales. However, the droplet radius is converted to be dimensionless with respect to its initial radius.

$$\frac{dX_{i,k}}{dt} = V_{i,k} \tag{6}$$

$$\frac{dV_{i,k}}{dt} = \frac{3}{4}\frac{\mu C_d}{\rho_k d_k^2}\mathrm{Re}_k \left(U_i - V_{i,k}\right) + g \tag{7}$$

$$\dot{m}_k = -\pi d_k Nu_k \frac{\lambda_s}{C_{ps}} \ln\left[1 + \frac{C_{ps}\left(T_g - T_k\right)}{L}\right] \tag{8}$$

$$\dot{m}_k = -\pi d_k Nu_k D_s \rho_s \ln\left[1 + \frac{Y_{vs} - Y_{vg}}{1 - Y_{vs}}\right] \tag{9}$$

where Nu_k is the Nusselt number of heat convection, which is determined as

$$Nu_k = 2 + 0.5\mathrm{Re}_k^{0.5} \tag{10}$$

and Re_k is the Reynolds number of droplet-gas relative motion, defined as

$$\mathrm{Re}_k = \frac{\rho\left|\vec{U} - \vec{V}_k\right| d_k}{\mu} \tag{11}$$

and Y_{vs} is the mass fraction of fuel vapor at the surface of droplet

$$Y_{vs} = B_v \exp(-E_v / RT_k) \tag{12}$$

and Y_{vg} is the mass fraction of fuel vapor in the computational cell.

$$\frac{d\left(d_k^2\right)}{dt} = -\frac{2Nu_k \lambda_s}{\rho_k C_{ps}} \ln\left[1 + \frac{C_{ps}\left(T_g - T_k\right)}{L}\right] \tag{13}$$

The momentum exchange between the gas-phase and the droplet is occurred due to the drag force and an empirical drag coefficient is applied in the present study. It can be expressed as

$$\beta_k = \frac{3}{4}C_d \frac{\rho\left|\vec{U} - \vec{V}_k\right|}{d_k} \tag{14}$$

where C_d is drag coefficient based on different Reynolds number given by

$$C_d = \begin{cases} \dfrac{24}{\mathrm{Re}_k}\left(1 + \dfrac{1}{6}\mathrm{Re}_k^{0.667}\right); & \mathrm{Re}_k < 1000 \\ 0.44; & \mathrm{Re}_k \geq 1000 \end{cases} \tag{15}$$

The droplet evaporation rate depends mainly on heat and mass transfer, and the evaporation latent heat. Based on stagnant film theory, heat transfer between the droplet and gas-phase is given by

$$Q_k = \pi d_k Nu_k \lambda_s \left(T_g - T_k\right)\frac{B_k}{\exp(B_k) - 1} \tag{16}$$

where B_k is a transfer number given by

$$B_k = \frac{-\dot{m}_k C_{ps}}{\pi d_k Nu_k \lambda_s} \tag{17}$$

In the droplet equation, the thermal enthalpy is defined as $h_k = C_{ps}T_k$

4. Solution Procedure

The governing equations of the gas phase are solved using the TEACH computational procedure of Patankar[13], where the finite difference approximations of the derivatives with respect to the space variables are obtained by integrating the equations over a control volume surrounding the nodes of the difference mesh. The numerical integration of the equation is carried over the staggered mesh with the grid nodes for the velocity components located in the middle of the faces of the scalar variable control volume. The solution procedure of TEACH does not solve the continuity equation directly. Instead the continuity equation is satisfied indirectly by an iterative scheme known as the SIMPLE algorithm of Patankar and Spalding [13]. The velocities are first calculated from the momentum equations using a guessed pressure distribution; then the pressure distribution is adjusted so that the velocities satisfy the mass continuity equation. The whole cycle is repeated. Appropriate modifications are made to the TEACH computer code to account for the additional source terms introduced as a result of the gas phase and liquid phase interaction and the unsteady terms of the gas-phase equations.

The liquid-phase equations are advanced in time by an explicit second-order Runge-Kutta method required a small time step. The numerical integration of these ordinary differential equations is relatively inexpensive compared to the solution of the gas-phase equations in terms of the computational time required. The liquid-phase and gas-phase equations are integrated with different time steps in order to exploit fully the advantage offered by the implicit TEACH procedure used for gas phase equations, which allows the numerical integration to be carried over a large time step. Based on the known gas phase properties the liquid phase equations are first advanced in the time from the n-th time level to the (n+1)-th time level corresponding to the gas phase time step Δt_g.

The gas phase equations are solved next. The solution procedure for the integration of the governing equations requires; (1) interpolation of the gas phase properties from the fixed Eulerian locations to the characteristic location; (2) integration of the liquid phase equations over a time step $\Delta t_{l,m}$; (3) redistribution of the source terms evaluated at the characteristic location among the Eulerian nodes

surrounding the characteristic; (4) Steps (1)-(3) are repeated until the liquid phase equations are advanced over a time step Δt_g. The characteristic locations as well as the gas phase properties are updated at the end of each time step $\Delta t_{l,m}$. Such a procedure is useful when the particles experience steep gradients. In the situations encountered otherwise it would be more appropriate to choose the characteristic location to be an average of the n-th and (n+1)-th time levels and thereby avoiding excessive computations involving interpolations. This aspect will be given future consideration along with the problem of choosing the optimum values needed for $\Delta t_{l,m}$ and Δt_g in order to enhance the rate of convergence in the steady-state calculations; (5) solve the gas phase equations. Steps (1)-(5) are repeated until the iterations converge before advancing to the next step for unsteady calculations. In the case of steady-state calculations the solution can be directly advanced to the next time step without the need for iteration.

The interpolation scheme required in Steps (1) and (3) is a linear second order accurate procedure. Figure 1 shows a grid cell surrounding a characteristic for the dependent variable ϕ. The gas phase properties at the characteristic location are interpolated as follows;

$$\phi_{g,char} = (\phi_g(I,J) \times \text{Vol?} + \phi_g(I,J+1) \times \text{Vol?}$$
$$+ \phi_g(I-1,J+1) \times \text{Vol?} \tag{18}$$
$$+ \phi_g(I-1,J) \times \text{Vol?}) / (\text{Cell volume})$$

The source term at the grid nodes due to liquid phase interaction is given by

$$s_{\phi,m}(I,J) = \frac{s_{\phi,char} \times \text{Vol?}}{\text{Cell volume}} \tag{19}$$

and $s_{\phi,m}(I,J+1)$, $s_{\phi,m}(I-1,J+1)$, and $s_{\phi,m}(I-1,J)$ are determined in a similar way. The contribution of the source terms $s_{\phi,lm}$ corresponds to a time step of $\Delta t_{l,m}$. The total contribution of these source terms over a time step Δt_g is given by

$$s_{\phi,l} = \sum_{m=1}^{M} \frac{\Delta t_{l,m}}{\Delta t_g} s_{\phi,lm} \tag{20}$$

where

$$\sum_{m=1}^{M} \Delta t_{l,m} = \Delta t_g \tag{21}$$

Depending on the relative location of the characteristic within the grid cell of a scalar dependent variable, the different grid cells of axial and radial velocity components are affected by the interpolation procedure because of the use of a staggered grid in the TEACH computational procedure.
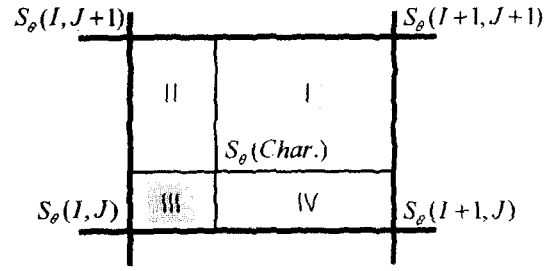

Figure 1 Grid cell surrounding a characteristic

5. Injection of the Particles

The mass flow rate of the fuel is determined from the stoichiometric conditions.

$$M_f = \frac{0.21 \Phi M_a W_f}{v W_o} \tag{22}$$

The injection time interval for a new characteristic to appear is based on the (Δx =) Eulerian mesh size and ($V_{k,0}$ =) injection velocity of the droplet. This ensures that the droplet properties are resolved on a commensurate scale with the gas-phase properties

$$dt_{injection} = \frac{\Delta x}{V_{k,0}} \tag{23}$$

The number of droplets in each characteristic is given by

$$n_k = L_k^3 \frac{M_{f,k} dt_{injection}}{(\frac{4}{3} \pi r_k^3 \rho_k)} \tag{24}$$

where

$$M_f = \sum M_{f,k} \tag{25}$$

At the injection time, the initial properties of the droplet such as $r_{k,0}$ and $T_{k,0}$, the droplet velocity $V_{k,0}$, and the half cone angle θ are specified. When 99 percent of the mass has been evaporated the characteristic is removed from the combustor and the remaining fuel is added as vapor instantaneously.

6. Result and Discussion

The numerical model is applied to simulate the isothermal flow and transverse injecting spray combustion in the axisymmetric sudden-expansion combustor. Figure 2 shows that the gas-phase velocity vectors. The air enters the combustor with velocity of 30 m/s, assumed to be laminar flow. The fuel is injected in the radial direction into the combustor at the beginning of the air entrance shown in the figure. There is a large recirculation zone in the near wall region behind the sudden-expansion step. This recirculation zone enhances the spray ignition and the flame stabilization.

The droplet trajectories are shown in Fig. 3. In the figure, three droplet groups can be identified by the size of the symbol representing the characteristic

location. The droplets travel along its own trajectories before the drag force causes the droplets to decelerate. Eventually, the droplets become to have the same directional path as the gas phase flow. Since most of the droplets vaporize near the injector, the excessive concentration of fuel vapor occurs near the injection source. The combustion proceeds further to the downstream region along the shear layer. The most intense combustion region is located close to the end of the combustor near the axis of symmetry. The low temperature of the recirculation region results form the cooling effect of the vaporization process.

Table 2 Values used in the computation

Parameter	Value
Inflow conditions of the combustor	
Velocity, U_c	30 m/s
Temperature, T_c	1000 K
Pressure, P_c	10 atm
Density, ρ_c	3.399 kg/m^3
Turbulent kinetic energy, k_c	0.03 m^2/s^2
Turbulent dissipation rate, ε	$\dfrac{k_c C_\mu^{0.75}}{0.0009}$
Duct wall temperature	700 K
Initial conditions of the liquid spray	
Fuel	n-decane
Liquid density, ρ_k	773 kg/m^3
Droplet temperature, T_k	300 K
Droplet velocity, V_k	200m/s

7. Conclusions

The numerical model for the spray combustion has been developed using the Eulerian-Lagrangian method. The calculation results have demonstrated that droplet vaporization, turbulent mixing, and energy conversion play important roles in various aspects of the combustor performance. While the simulation has to be validated with the experimental results, the calculation results seem to have a good tendency of gas-phase and droplet properties in the practical combustor environment. The current numerical method has an error associated with the models used for turbulence, combustion, vaporization, and idealization of spray injection process. The accuracy of the vaporization model could be improved by considering the effects associated with physical property variations. Further investigation could be continued to reduce the associated error and to validate the numerical method with experimental results.
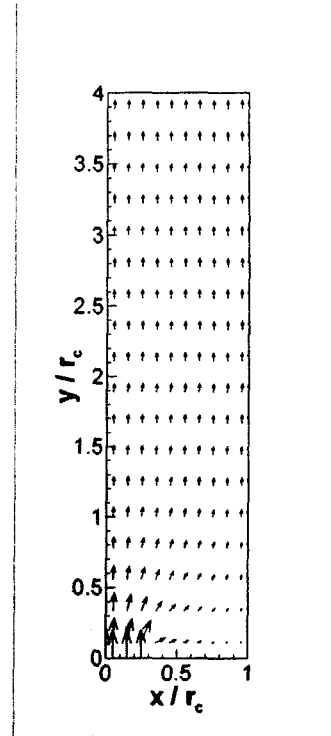
Figure 2 Gas-phase velocity vectors (isothemal flow)
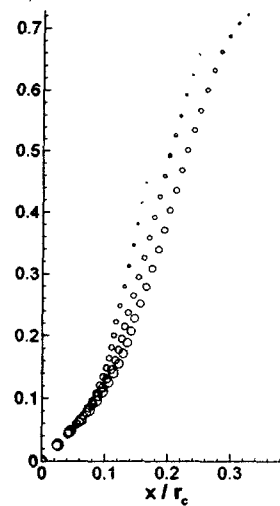
Figure 3 Droplet trajectory & size distribution

References

1) Law, C. K. : Recent Advances in Droplet Vaporization and Combustion, *Prog. Energy Combust. Sci. 8, ,1978,* pp. 171-201.

2) G . M. Faeth, : Evaporation and Combustion of spray, *Prog. Energy Combus. Sci. Vol. 9,* 1983,pp. 1-76

3) G. M. Faeth, : Current Status of Droplet and Liquid Combustion, *Prog. Energy Combust. Sci., Vol 3,* 1977, pp. 191-224

4) W. A. Sirignano, : Fuel Droplet Vaporization and Spray Combustion, *Prog. Energy Combust. Sci.,Vol 9,* 1983, pp. 291-322

5) W. A. Sirignano, : The Formulation of Spray Combustion Models: Resolution Compared to Droplet Spacing, *ASME Journal of Heat Transfer, Vol 108, No 3,* 1986, pp. 633-639

6) C. T. Crown, M. P. Sharma, and D. E. Stock, " The Particle-Source-in -Cell(PSIC) Model for Gas-Droplet flow", *ASME J, Vol 18,* pp 1503-1510.

7) Shuen, Jian-Shun : Prediction of the structure of fuel spray in cylindrical combustion chambers, *Journal of propulsion and power, v.3 no.2,* 1987, pp.105-113

8) Gould, Richard D. Stevenson, Warren H. Thompson, H. Doyle : Simultaneous velocity and temperature measurements in a premixed dump combustor , *Journal of propulsion and power, v.10 no.5,* 1994, pp.639-645

9) Launder, B. E., Spalding, D. B., : *Mathematical Models of Turbulence,* Academic Press, London, United Kingdom, 1972.

10) Spalding, D. B. : Mathematical Model of Turbulence Flames : A review , *Combustion Science and Technology, Vol. 13,* 1976, pp.3-25

11) Westbrook, C. K, Dryer, F. L., : Chemical Kinetic Modeling of Hydrocarbon Combustion, *Prog. Energy Combust. Sci. Vol. 10,* 1984, pp. 1-57

12) CRC : *Handbook of Physics and Chemistry,* Chemical Rubber Co., Cincinnati, OH, 1985.

13) Partankar, S. V., : *Numerical Heat transfer and Fluid Flow,* Hemisphere, Washington, D.C, 1980

U = gas-phase velocity

V = droplet velocity

W = reaction rate

Y = species mass fraction

α_N = fuel nitrogen content of spray droplets

β_k = gas-droplet flow drag coefficient

Γ_ϕ = exchange coefficient in equation (1)

ε = dissipation of energy

μ = viscosity

ν = stoichiometric ratio

ρ = density

Φ = equivalence ratio

subscripts

g = gas-phase

i, j, k = coordinate direction

k = k -group droplet phase

s = surface layer of droplet

T = turbulence

Nomenclature

a = exponents of fuel mole fraction in equation (2)

b = exponents of oxidizer mole fraction in equation (2)

C_d = drag coefficient between gas and droplet

C_1, C_2, C_μ = empirical constant of gas-phase $k - \varepsilon$ turbulence model

D = diffusion coefficient

h = enthalpy

k = kinetic energy of turbulence

L = latent heat

$\dot{m}_k$ = droplet vaporization rate

M = molecular weight

n = droplet number density

Re_k = relative Reynolds number

T = temperature